



**HAL**  
open science

## The origin of Bohm diffusion, investigated by a comparison of different modelling methods

E Bultinck, S Mahieu, D Depla, A Bogaerts

► **To cite this version:**

E Bultinck, S Mahieu, D Depla, A Bogaerts. The origin of Bohm diffusion, investigated by a comparison of different modelling methods. *Journal of Physics D: Applied Physics*, 2010, 43 (29), pp.292001. 10.1088/0022-3727/43/29/292001 . hal-00569653

**HAL Id: hal-00569653**

**<https://hal.science/hal-00569653>**

Submitted on 25 Feb 2011

**HAL** is a multi-disciplinary open access archive for the deposit and dissemination of scientific research documents, whether they are published or not. The documents may come from teaching and research institutions in France or abroad, or from public or private research centers.

L'archive ouverte pluridisciplinaire **HAL**, est destinée au dépôt et à la diffusion de documents scientifiques de niveau recherche, publiés ou non, émanant des établissements d'enseignement et de recherche français ou étrangers, des laboratoires publics ou privés.

# The origin of Bohm diffusion, investigated by a comparison of different modeling methods.

**E Bultinck<sup>1</sup>, S Mahieu<sup>2</sup>, D Depla<sup>2</sup>, A Bogaerts<sup>1</sup>**

<sup>1</sup> Research group PLASMANT, Department of Chemistry, University of Antwerp, Universiteitsplein 1, 2610 Antwerp, Belgium

<sup>2</sup> Research group DRAFT, Department of Solid State Sciences, Ghent University, Krijgslaan 281 (S1), B-9000 Gent, Belgium

E-mail: [evi.bultinck@ua.ac.be](mailto:evi.bultinck@ua.ac.be)

## **Abstract.**

“Bohm diffusion” causes the electrons to diffuse perpendicular to the magnetic field lines. However, its origin is not yet completely understood: low and high frequency electric field fluctuations are both named to cause Bohm diffusion. The importance of including this process in a Monte Carlo (MC) model is demonstrated by comparing calculated ionization rates with particle-in-cell/Monte Carlo collisions (PIC/MCC) simulations. A good agreement is found with a Bohm diffusion parameter of 0.05, which corresponds well with experiments. Since the PIC/MCC method accounts for fast electric field fluctuations, we conclude that Bohm diffusion is caused by fast electric field phenomena.

PACS numbers: 52.25 Xz, 52.25.Fi, 52.65 Pp, 52.65 Rr

Submitted to: *J. Phys. D: Appl. Phys.*

Magnetron devices are widely applied for the sputter deposition of thin films. In magnetron discharges, both an electric and a magnetic field are present. The magnetic field causes the electrons to be trapped close to the cathode, leading to a more efficient use of the electrons to ionize the gas atoms. In this way, higher power densities can be achieved as compared to a non-magnetized glow discharge, resulting in enhanced sputtering of the target. However, experimental and computational observations show that electron transport perpendicular to the magnetic field lines is higher than expected from classical theory [1–4]. This anomalous electron diffusion is commonly attributed to instabilities in the discharge. Indeed, temporary electric field changes can push electrons away from their magnetic traps, and therefore enhance electron transport across the magnetic field lines. However, the origin of these instabilities is still subject to discussion. Indeed, according to [5–7], low frequency field oscillations (in the order of kHz) are the origin of Bohm diffusion, whereas also high frequency oscillations (in the order of MHz) are reported to cause anomalous diffusion [8, 9]. Therefore, this work is dedicated to the effect and the interpretation of anomalous diffusion.

To study the electron movement in magnetron discharges, numerical simulations are applied. The clearly non-Maxwellian electron energy distribution in magnetron discharges caused by the low pressure, makes particle modeling, such as Monte Carlo (MC) and particle-in-cell/Monte Carlo collisions (PIC/MCC) simulations, the most suitable technique. Here, each electron is followed individually. The electrons move in the electric and magnetic fields according to Newton’s equations of motion. Furthermore, they collide probabilistically in the Monte Carlo algorithm, and interactions with the walls are also accounted for (i.e. electron reflection, adsorption and emission).

Since the magnetic field is not much influenced by the charged plasma species, it is typically used as input in such models. In a MC model, the electric field is used as input as well. Hence it is a non self-consistent modeling approach, which has the advantage of a relatively short calculation time, but in expense, it does not account for electric field variations due to charge fluctuations. As a consequence, the effect of Bohm diffusion must be explicitly included in a MC model. On the other hand, in a PIC/MCC model, the electric field is recalculated in each time step by means of the Poisson equation. Therefore, the PIC/MCC model implicitly accounts for electric field changes caused by the charged particles, and hence for possible anomalous diffusion. An important remark here is that large time scale oscillations can however not be modeled with a PIC/MCC method due to calculation time limitations. Indeed, a typical low frequency oscillation of 100 kHz corresponds to 10  $\mu$ s per oscillation, acquiring a calculation time of months when simulating a couple of oscillations. In other words, with a PIC/MCC model we are only able to investigate whether high frequency fluctuations (i.e. above 100kHz) cause Bohm diffusion.

In the present work, we have performed simulations with both a PIC/MCC model and a MC model, to investigate the importance and origin of Bohm diffusion. A detailed explanation of the PIC/MCC model used in this work can be found in [10,11]. The MC model is based on the same principles, and hence, it will not be explained in detail here. The main differences are that the electric field is not calculated self-consistently. Moreover, only electrons are followed, and therefore only electron impact collisions are included, whereas in a PIC/MCC model also other plasma species are followed [10,11]. Here, we will only focus on the treatment of Bohm diffusion in the MC model.

In fluid models, Bohm diffusion is included by using a Bohm diffusion coefficient in the electron balance equations [2,3], or by using an adjusted magnetic field based on the Bohm diffusion coefficient expression [12]. However, in particle models, diffusion coefficients are not applied, so anomalous diffusion must be included differently. Bohm diffusion can be seen as an interaction of an electron with the electric field fluctuations, which knocks the electron away from the magnetic field line. Therefore, in our MC model, this effect is included as an extra collision event with a frequency  $f_{Bohm}$ , proportional to the gyrofrequency  $f_g$  [9].

$$f_{Bohm} = K_{Bohm} f_g \quad (1)$$

The gyrofrequency  $f_g = \frac{qB}{2\pi m}$ , with  $q$  the elementary charge,  $m$  the electron mass, and  $B$  the magnitude of the magnetic field vector. The proportionality factor,  $K_{Bohm}$ , is called the Bohm parameter and can be adapted in the model so that the calculated electron properties agree with results from self-consistent calculations and/or experiments.

The probability of this ‘‘Bohm collision’’ event is:

$$P_{Bohm} = 1 - \exp(-\Delta t f_{Bohm}) \quad (2)$$

If Bohm diffusion occurs, electrons are assumed to scatter preferably in the direction perpendicular to the magnetic field [9]. Therefore, the post-collision velocity is derived by rotating the perpendicular component of the velocity vector with respect to  $\mathbf{B}$  with an arbitrary angle, and leaving the parallel component unchanged. In the present study, a planar circular magnetron is investigated. Because of the cylindrically symmetrical reactor, the magnetic field can be described in two-dimensions ( $B_r, B_z$ ), but the species velocities are three-dimensional ( $v_r, v_\theta, v_z$ ) to describe properly the electron gyration around the magnetic field lines, and to satisfy the energy conservation. Therefore, the parallel velocity vector,  $\mathbf{v}_\parallel$ , represents the vector parallel to  $\mathbf{B}$ , lying in the  $r - z$  plane. Consequently, since  $\mathbf{v}$  also has a  $\theta$  component, the perpendicular velocity vector,  $\mathbf{v}_\perp$ , lies in the  $r - \theta - z$  plane. It is hence  $\mathbf{v}_\perp$  which needs to be rotated.

To find the components of  $\mathbf{v}_\perp$ , the  $r - z$  reference frame is rotated so that the new  $r$ -axis lies parallel to  $\mathbf{B}$ . With  $\chi$  the angle between  $\mathbf{v}$  and  $\mathbf{B}$ ,  $\cos \chi = \frac{\mathbf{v} \cdot \mathbf{B}}{v \cdot B}$ . Since  $\mathbf{v} = \mathbf{v}_\parallel + \mathbf{v}_\perp$ , the components of the velocity vector perpendicular to  $\mathbf{B}$ ,  $\mathbf{v}_\perp$ , in the new reference frame are:

$$\begin{aligned} v_{r,\perp} &= v_r - \frac{v \cos \chi}{B} \cdot B_r \\ v_{\theta,\perp} &= v_\theta \\ v_{z,\perp} &= v_z - \frac{v \cos \chi}{B} \cdot B_z \end{aligned} \quad (3)$$

When rotating  $\mathbf{v}_\perp$  around the new  $r$ -axis, its new velocity components are:

$$\begin{aligned} v'_{r,\perp} &= v_{r,\perp} \\ v'_{\theta,\perp} &= v_{\theta,\perp} \cos(2\pi RN) - v_{z,\perp} \sin(2\pi RN) \\ v'_{z,\perp} &= v_{\theta,\perp} \sin(2\pi RN) + v_{z,\perp} \cos(2\pi RN) \end{aligned} \quad (4)$$

Finally, since  $\mathbf{v}' = \mathbf{v}_{\parallel} + \mathbf{v}'_{\perp}$ , returning to the original reference frame gives the velocity after a Bohm collision:

$$\begin{aligned} v'_r &= v_r \\ v'_\theta &= v'_{\theta,\perp} \\ v'_z &= \frac{v \cos \chi}{B} \cdot B_z + v'_{z,\perp} \end{aligned} \quad (5)$$

The investigated balanced planar circular magnetron has a cathode target with a radius of 25 mm, in a cylindrical chamber with walls at 28 mm from the symmetry axis. Parallel to the target, a substrate is located at a distance of 24 mm from the target, as presented in [13,14]. The magnetron operates at a gas temperature of 300 K, an argon pressure of 1 Pa and an oxygen pressure of 0.24 Pa. The applied magnetic field has a maximum radial magnetic field strength of 1040 G. In the PIC/MCC model, the electric field is generated by an external voltage of -600 V, the resistance of this external circuit is 1500  $\Omega$ , giving rise to a cathode voltage of -312 V and a current of 0.2 A. The self-consistently calculated electric field is used as input for the MC model. Since this self-consistently calculated electric field considerably changes in time (see further), it is smoothed in time at steady state to be used as input in the MC model. Moreover, to avoid low energy electrons to get trapped in local electric field maxima, only fast electrons are followed in the MC model.

In the MC model, we varied the Bohm parameters  $K_{Bohm}$  from 0 (i.e. no Bohm diffusion) to 0.01, 0.03, 0.05 and 0.1. In figure 1, the electron impact ionization rate of argon, calculated with these Bohm parameters, is presented. Since only fast electrons are followed in the MC model, we use the electron impact ionization rate rather than the (fast) electron density to evaluate Bohm diffusion. The ionization rate gives us an idea on the location of both fast and slow electrons (created by these ionizations), whereas the electron density only shows the location of the fast electrons. From figure 1 it is clear that an increased Bohm parameter causes the ionization rate profile to spread out towards the bulk, and hence the maximum is lower. Indeed, increasing the Bohm parameter enhances the electron mobility, causing the electrons to escape from their magnetic traps towards the bulk. This leads to a more spread out gas ionization. These results are in correspondance to [9].

A PIC/MCC calculation was carried out for the same conditions, and the ionization rate profile is presented in figure 2. This profile differs considerably from the profile calculated with the MC model without explicitly including Bohm diffusion ( $K_{Bohm} = 0$ ): the maximum is lower, and the profile is more spread out than the MC profile. This indicates that Bohm diffusion is already present at fast electric field fluctuations, because the self-consistent PIC/MCC calculation only accounts for electric field fluctuations at a short time scale. These electric field fluctuations are apparent in figures 3 and 4, presenting the z-component of the electric field ( $\mathbf{E}_z$ ), calculated with the PIC/MCC model (since  $\mathbf{E}_r$  is approximately 10 times smaller, these results are not shown here). Figure 3 shows the spatial profile of  $\mathbf{E}_z$ , which has changed at three different time steps. Moreover, figure 4 clearly demonstrates the electric field fluctuations in a time interval of 2  $\mu s$  in a grid point in the sheath (at  $r=13.5$  mm,  $z=0.2$  mm) and in the bulk (at  $r=13.5$  mm,  $z=20$  mm), which indeed occur at short time scales (i.e. high frequency). The electric field in the sheath does not vary so much (compared to its absolute value) but the fluctuations in the plasma bulk are very pronounced.

When the Bohm parameter is increased in the MC model, the shape of the profile calculated with the MC model matches the one calculated with the PIC/MCC model much better. However, the maxima of the MC profiles decrease below the maximum of the PIC/MCC profile. This is probably caused by the fact that in the MC model, only electron impact collisions are included. In reality, other ionization collisions, such as  $\text{Ar}^+$  ion and fast Ar atom impact ionization, can also be important [15] and they are explicitly included in the PIC/MCC model [10, 11]. Moreover, the PIC/MCC results indeed showed that a considerable fraction of all ionization reactions can be ascribed to  $\text{Ar}^+$  ion and fast Ar atom impact. Therefore, it is logical that the electron density and the electron impact ionization rate as calculated with the MC model are lower than the PIC/MCC results. Therefore, we will only compare the shape of the profiles and not the absolute values.

In figure 5 the electron impact ionization rates, normalized to its maximum value, on a line above the race track ( $r=13.5$  mm) are compared. This figure shows that a Bohm parameter of 0.05 reproduces the shape of the PIC/MCC profile best. This value lies in the range of the experimentally obtained local Bohm parameters of  $1/6 - 1/25$  (0.17 - 0.04) [1]. Since the PIC/MCC calculation can only track short time scale electric field instabilities because of the limited calculation time, we can conclude that Bohm diffusion is mainly caused by high frequency electric field instabilities (i.e. below  $10 \mu\text{s}$ , equivalent to a minimum of 100 kHz).

In summary, this letter describes the treatment of Bohm diffusion in a two-dimensional cylindrical MC model. Bohm diffusion is included as an extra collision event, and afterwards, the velocity component of the electron perpendicular to the magnetic field line is scattered with a random angle. Anomalous electron diffusion across the magnetic field lines is caused by electric field instabilities, which draw the electrons away from their magnetic traps, and enhance their mobility. A self-consistent PIC/MCC model implicitly includes short time scale electric field variations. By tuning the Bohm parameter so that the calculated normalized ionization rate of the MC model is comparable with the PIC/MCC model, a Bohm parameter of 0.05 gives the best agreement (note that the absolute values can not be compared due to certain omitted electron producing collisions, e.g.  $\text{Ar}^+$  ion and fast Ar atom impact ionizations). From experiments [1], Bohm parameters in the range of 0.04 - 0.17 were found. Since the experimental values correspond well to our derived Bohm parameter, we can conclude that Bohm diffusion is mainly caused by fast electric field fluctuations.

Moreover, this implies that in a PIC/MCC model, Bohm diffusion is implicitly and completely included. However, by using a MC model, the calculation time is tremendously lower (i.e. a few days compared to three weeks to obtain statistically valid results and to reach convergence). Therefore, when including Bohm diffusion explicitly in the MC model, we will be able to model large scale reactors and complex geometries, which is impossible with a PIC/MCC model due to the very large calculation time of these simulations.

## Acknowledgments

This work is supported by a joint IWT (SBO 60030) project and a FWO project of both research groups. S. Mahieu is indebted to the FWO Flanders for financial support. The computer facility CalcUA from the University of Antwerp is acknowledged.

## References

- [1] J W Bradley, S Thompson, and Y A Gonzalvo. Measurement of the plasma potential in a magnetron discharge and the prediction of the electron drift speeds. *Plasma Sources Sci. Technol.*, 10(3):490, 2001.
- [2] G Lister. Influence of electron diffusion on the cathode sheath of a magnetron discharge. *J. Vac. Sci. Technol. A.*, 14(5):2736, 1996.
- [3] J W Bradley, R D Arnell, and D G Armour. Measurement and modelling of the bulk plasma in magnetron sputtering sources. *Surf. Coat. Technol.*, 97(1-3):538, 1997.
- [4] S M Thompson and J W Bradley. The effect of rotating cylindrical Langmuir probes in magnetron plasmas. *Contrib. Plasm. Phys.*, 41(5):481, 2001.
- [5] T A van der Straaten and N F Cramer. Transverse electric field and density gradient induced instabilities in a cylindrical magnetron discharge. *Phys. Plasmas*, 7:391, 2000.
- [6] E Martines, R Cavazzana, G Serianni, M Spolaore, and L Tramontin. Electrostatic fluctuations in a direct current magnetron sputtering plasma. *Phys. Plasmas*, 8:3042, 2001.
- [7] O Bilyk, M Holik, A Marek, P Kudrna, M Tichy, and J F Behnke. Fluctuations of the magnetically-supported dc discharge in coaxial configuration. *Vacuum*, 76:437, 2004.
- [8] A R Pal, J Chutia, and H Bailung. Observation of instability in presence of ExB flow in a direct current cylindrical magnetron discharge plasma. *Phys. Plasmas*, 11:4719, 2004.
- [9] A Smirnov, Y Raitses, and N J Fisch. Electron cross-field transport in a low power cylindrical Hall thruster. *Phys. Plasmas*, 11:4922, 2004.
- [10] E Bultinck, S Mahieu, D Depla, and A Bogaerts. The reactive sputter deposition of a TiN film, simulated with a particle-in-cell/Monte Carlo collisions model. *New J. Phys.*, 11:023039, 2009.
- [11] E Bultinck, S Mahieu, D Depla, and A Bogaerts. Particle-in-cell/Monte Carlo collisions treatment of an Ar/O<sub>2</sub> magnetron discharge used for the reactive sputter deposition of TiO<sub>x</sub> films. *New J. Phys.*, 11:103010, 2009.
- [12] P Tomason, P Browning, and J Bradley. 1-D self-consistent fluid modelling of the pulsed magnetron discharge. *Plasma Process. Polym.*, 6:S767, 2009.
- [13] E Bultinck, I Kolev, A Bogaerts, and D Depla. The importance of an external circuit in a particle-in-cell/monte carlo collisions model for a direct current planar magnetron. *J. Appl. Phys.*, 103:013309, 2007.
- [14] D Depla, G Buyle, J Haemers, and R De Gryse. Discharge voltage measurements during magnetron sputtering. *Surf. Coat. Technol.*, 200:4329, 2006.
- [15] A Bogaerts and R Gijbels. The role of fast argon ions and atoms in the ionization of argon in a direct-current glow discharge: a mathematical simulation. *J. Appl. Phys.*, 78(11):6427, 1995.

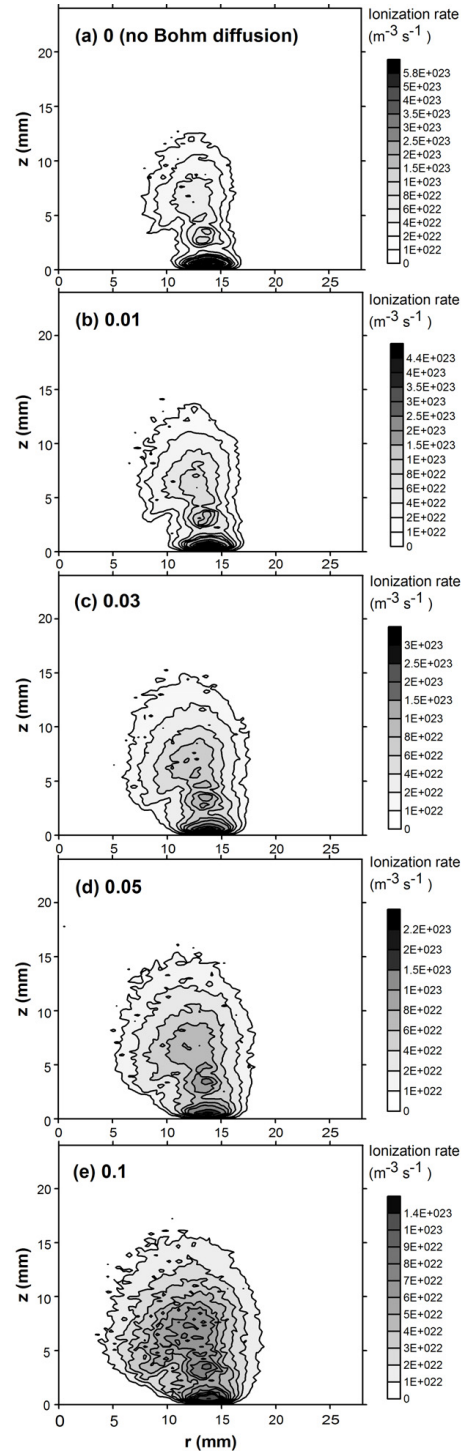


**Figure 1.** Electron impact ionization rates of Ar (in  $\text{m}^{-3} \text{s}^{-1}$ ), calculated with the MC model, with different Bohm parameters of (a) 0, (b) 0.01, (c) 0.03, (d) 0.05 and (e) 0.1. The calculated electric field of the PIC/MCC model is used as input (with a cathode voltage of -312 V and a cathode current of 0.2 A). The magnetron operates at an Ar pressure of 1 Pa and an  $\text{O}_2$  pressure of 0.24 Pa. The  $z$ -axis corresponds to the symmetry axis of the cylindrically symmetrical reactor.

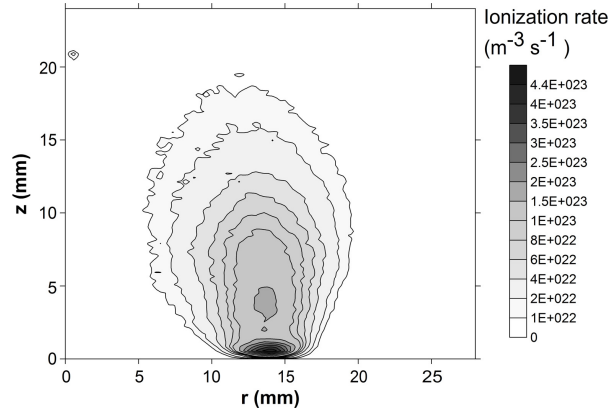


**Figure 2.** Electron impact ionization rate of Ar (in  $\text{m}^{-3} \text{s}^{-1}$ ), calculated with the PIC/MCC model, for the same conditions as in figure 1. The  $z$ -axis corresponds to the symmetry axis of the cylindrically symmetrical reactor.

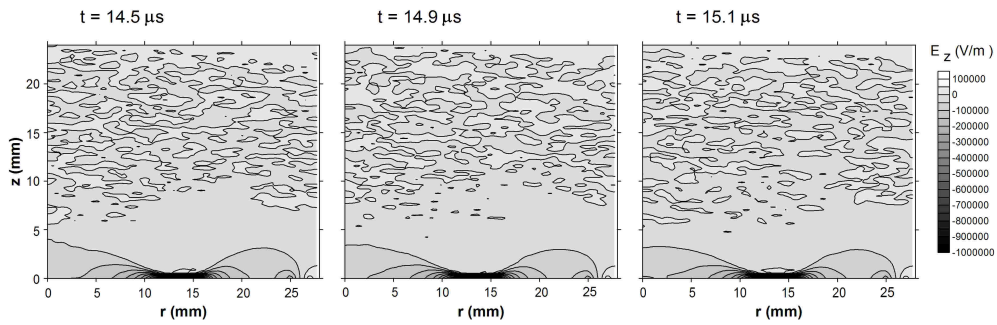


**Figure 3.** Spatial profile of the  $z$ -component of the electric field ( $E_z$ ) at three different time steps, calculated with the PIC/MCC model. The electric field in the sheath is more or less the same, but the fluctuations in the bulk are very pronounced.

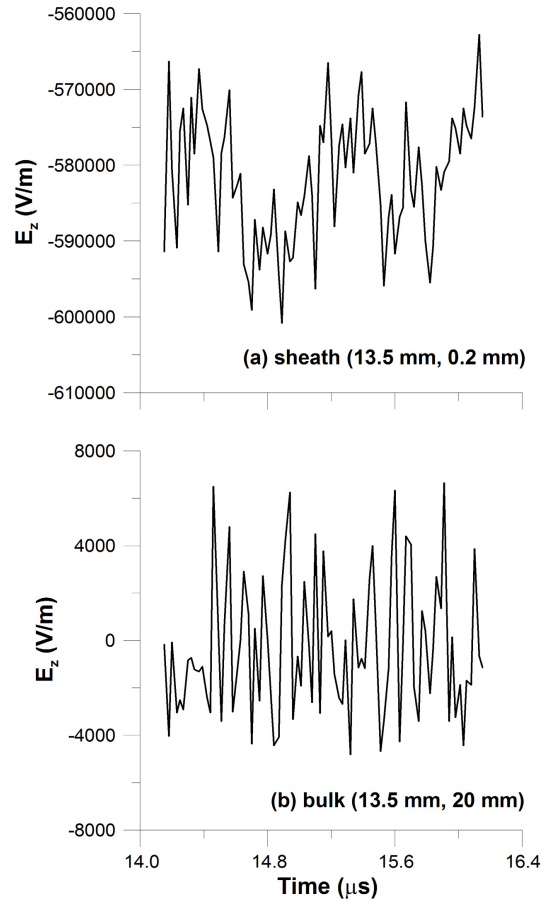


**Figure 4.** Fluctuations of the  $z$ -component of the electric field ( $\mathbf{E}_z$ ) in a time interval of  $2 \mu\text{s}$  in a grid point (a) in the sheath (at  $r=13.5 \text{ mm}$ ,  $z=0.2 \text{ mm}$ ) and (b) in the bulk (at  $r=13.5 \text{ mm}$ ,  $z=20 \text{ mm}$ ), calculated with the PIC/MCC model.

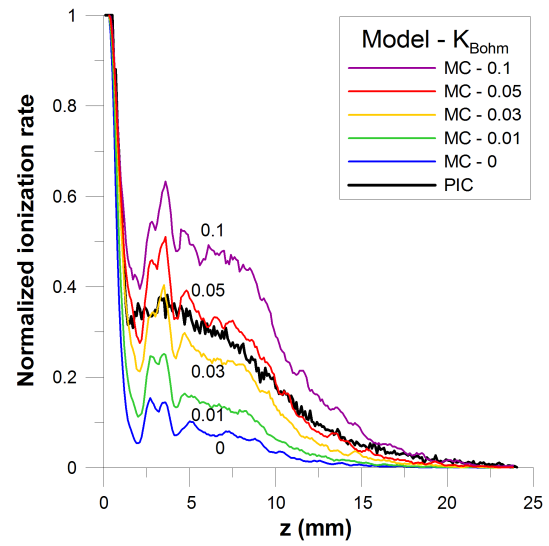


**Figure 5.** (Color online) Normalized electron impact ionization rates of Ar on a line above the race track ( $r=13.5$  mm), calculated with both models, as denoted in the legend.